Eur Radiol (2013) 23:2784–2792
DOI 10.1007/s00330-013-2891-1

MAGNETIC RESONANCE

Time-of-flight angiography: a viable alternative to contrast-enhanced MR angiography and fat-suppressed T1w images for the diagnosis of cervical artery dissection?

E. M. Coppenrath · N. Lummel · J. Linn · O. Lenz · M. Habs · K. Nikolaou · M. F. Reiser · M. Dichgans · T. Pfefferkorn · T. Saam

Received: 9 December 2012 / Revised: 29 March 2013 / Accepted: 3 April 2013 / Published online: 4 June 2013

Abstract
Objectives To compare the use of an unenhanced high-resolution time-of-flight MR angiography sequence (Hr-TOF MRA) with fat-suppressed axial/coronal T1-weighted images and contrast-enhanced angiography (standard MRI) for the diagnosis of cervical artery dissection (cDISS).
Methods Twenty consecutive patients (9 women, 11 men, aged 24–66 years) with proven cDISS on standard MRI underwent Hr-TOF MRA at 3.0 T using dedicated surface coils. Sensitivity (SE), specificity (SP), positive and negative predictive values (PPV, NPV), Cohen's kappa (κ) and accuracy of Hr-TOF MRA were calculated using the standard protocol as the gold standard. Image quality and diagnostic confidence were assessed on a four-point scale.
Results Image quality was rated better for standard MRI (P=0.02), whereas diagnostic confidence did not differ significantly (P=0.27). There was good agreement between Hr-TOF images and the standard protocol for the presence/absence of cDISS, with κ=0.95 for reader 1 and κ=0.89 for reader 2 (P< 0.001). This resulted in SE, SP, PPV, NPV and accuracy of 97 %, 98 %, 97 %, 98 % and 97 % for reader 1 and 93 %, 96 %, 93 %, 96 % and 95 % for reader 2.
Conclusions Hr-TOF MRA can be used to diagnose cDISS with excellent agreement compared with the standard protocol. This might be useful in patients with renal insufficiency or if contrast-enhanced MR angiography is of insufficient image quality.
Key Points
- *New magnetic resonance angiography sequences are increasingly used for vertebral artery assessment.*
- *A high-resolution time-of-flight sequence allows the diagnosis of cervical artery dissection.*
- *This technique allows the diagnosis without intravenous contrast medium.*
- *It could help in renal insufficiency or when contrast-enhanced MRA fails.*

Keywords Internal carotid artery dissection · Vertebral artery dissection · Angiography magnetic resonance · Apoplexy cerebrovascular · Contrast media

Abbreviations

cDISS	cervical artery dissection
CE-MRA	contrast-enhanced MR angiography
CNR	contrast-to-noise ratio
DSA	digital subtraction angiography
fs	fat-suppressed
Hr-TOF MRA	high-resolution time-of-flight MR angiography sequence
κ	kappa value

E. M. Coppenrath · O. Lenz · K. Nikolaou · M. F. Reiser · T. Saam (✉)
Institute for Clinical Radiology, Ludwig-Maximilians-University Hospital Munich, Pettenkoferstr. 8a, 80336 München, Germany
e-mail: tobias.saam@med.lmu.de

N. Lummel · J. Linn
Department of Neuroradiology, Ludwig-Maximilians-University Hospital Munich, München, Germany

M. Dichgans
Institute for Stroke and Dementia Research, Ludwig-Maximilians-University Hospital Munich, München, Germany

M. Habs · T. Pfefferkorn
Department of Neurology, Ludwig-Maximilians-University Hospital Munich, München, Germany

MIP	reconstruction maximum intensity projection
NPV	negative predictive value
PET-CT	combination of positron emission tomography and computed tomography
PPV	positive predictive value
SE	sensitivity
SNR	signal-to-noise ratio
SP	specificity

Introduction

Cervical artery dissection (cDISS) might be suspected in younger and middle-aged patients suffering a stroke. It can also be a cause of indefinite neurological symptoms (e.g. Horner syndrome [1] or headache/migraine [2]). Its pathophysiology is poorly understood and a variety of constitutional factors (e.g. Ehlers–Danlos or Marfan's disease), genetic predisposition [3] and environmental factors, such as major and minor trauma but also recent infection [4, 5] are associated with an increased risk of cDISS. Moreover, a recent study demonstrated that a subset of patients with spontaneous cDISS showed signs of a generalised transient inflammatory arteriopathy in contrast-enhanced carotid MRI and whole-body PET-CT [6].

Embolic stroke develops usually in the first few days after cDISS. Therefore, early and reliable diagnosis is of the utmost importance to start a timely treatment and to prevent serious complications. Clinical symptoms are manifold and often non-specific; for that reason, diagnosis relies heavily on imaging findings. Several studies have shown that MRI is ideally suited to the diagnosis of cDISS [7]. Fat-suppressed T1w images are able to depict hyperintense signal in the vessel wall, consistent with the vessel wall haematoma, the so-called crescent sign. MR angiography can detect occlusions or stenosis caused by the cDISS and often shows a relatively long narrowing of the vessel, the so-called string sign. However, contrast-enhanced MR angiography fails to reach sufficient image quality in up to 10 % of cases [8]. Moreover, contrast media application is associated with nephrogenic systemic fibrosis (NSF) in patients with renal insufficiency [9]. Thus alternative and/or additional imaging sequences that allow the diagnosis of cDISS without the use of contrast agents are desirable. A promising approach is the time-of-flight (TOF) sequence, which provides information about the vessel lumen and the vessel wall simultaneously [10, 11].

The aim of our study was to compare the diagnostic performance of an unenhanced time-of-flight MR angiography sequence (Hr-TOF MRA) using a dedicated four-channel carotid surface coil versus fat-suppressed axial/coronal T1-weighted images *and* contrast-enhanced angiography (standard MRI) with a standard head and neck coil for the diagnosis of cervical artery dissection.

Materials and methods

Patients

Patients with cDISS treated at our centre between August 2007 and August 2009 were included in the study if the following inclusion criteria were fulfilled:

1. Clinical suspicion and unequivocal evidence of cDISS on standard MRI (hyperintense signal on fat-suppressed T1w sequences demonstrating intramural methaemoglobin and stenosis or occlusion in contrast-enhanced MR angiography)
2. Written informed consent
3. Performance of standard MRI (T1w fat-suppressed images and contrast-enhanced MR angiography) and Hr-TOF MRA within 1 week

Case history and cardiovascular risk factors such as smoking, hypertension, hypercholesterolaemia, coronary heart disease, diabetes mellitus and positive family history were recorded (Table 1). The study was approved by the local institutional ethics committee and complied with the Declaration of Helsinki.

MRI

Initially patients underwent MR with a 1.5-T Symphony (Siemens Medical Solutions, Erlangen, Germany) or a 3.0-T GE device (Signa HDxt, GE Healthcare, Milwaukee, WI, USA) using a standard head and neck coil. Sequences included fat-suppressed (fs) T1w sequences with a slice thickness of 3.5 mm at 1.5 T (3.0 mm at 3.0 T) in coronal and axial planes and contrast-enhanced MR angiography (CE-MRA) with a pixel size of 0.84×0.84 mm^2 at 1.5 T and 1.0×1.0 mm^2 at 3.0 T (fs T1w and CE-MRA standard MRI). Coverage reached from the shoulders to the middle of the skull for the CE-MRA and from the carotid bifurcation to the carotid T for the fs T1w sequence. MIP reconstructions were carried out for representation of CE-MRA.

We defined Hr-TOF as a TOF sequence with high spatial resolution, high SNR (signal-to-noise ratio) and high CNR (contrast-to-noise ratio). The high SNR and CNR are achieved by the use of dedicated surface coils [13]. Hr-TOF MRA was carried out at 3 T (Verio, Siemens Medical Solutions, Erlangen, Germany) with a flexible four-channel carotid surface coil (Machnet BV, Eelde, Netherlands) using a PAT factor of 2 and a slice thickness of 1 mm [14]. The flexible surface coils are combined with the head coil in order to fully depict the V_4 segment of the vertebral artery.

Table 1 Patient characteristics

	Study population (n=20) Mean±SD (range) or %
Age, years	45.4±10.7
Male sex, %	55
BMI, kg/m^2	24.5±5.1
MR imaging	
Total occlusion, %	12.5
Stenosis in dissected vessels, %	TOF 66.9±22.4; T1w 63.5±29.3
Multiple dissections, %	40
Internal carotid artery dissection	
C_1 segment, %	56
C_2–C_7 segment, %	44
Vertebral artery dissection	
V_1 segment, %	0
V_2 segment, %	28.6
V_3 segment, %	42.8
V_4 segment, %	28.6
Symptoms	
Stroke, %	60
Horner's syndrome, %	5 (1 patient)
Unspecific head or neck pain, %	35
Cardiovascular risk factors	
Current smoker, %	25
Former smoker, %	25
Hypertension, %	25
Hypercholesterolaemia, %	25
Coronary heart disease	0
Diabetes, %	0
Family history of cardiovascular events, %	10

BMI body mass index

Classification of internal carotid artery (C_1–C_7) [12]

Coverage reached from the carotid bifurcation to the carotid T. Coronal MIP reconstructions of axial acquired Hr-TOF MRA images were obtained. MR acquisition time ranged from 4:11 to 6:17 min depending on the number of slabs required. MR parameters are described in detail in Table 2.

Image analysis

Two experienced (neuro)radiologists (E.C., J.L.) with more than 10 years of MR experience who were blinded to the clinical information reviewed the images independently from each other. Standard MRI and Hr-TOF were evaluated separately for the presence or absence of arterial dissection (yes/no) in both internal carotid arteries and both vertebral arteries. The degree of stenosis was measured according to the North American Symptomatic Carotid Endarterectomy Trial (NASCET) method. Image quality was rated as follows: 4=excellent, uniform image; 3=good, minimal heterogeneity, only minor flow artefacts; 2=satisfactory, delineated lumen, noticeable flow artefacts; 1=not suitable for diagnosis. Diagnostic confidence was rated as 4=excellent, exact diagnosis possible; 3=good, with definite diagnosis possible; 2=fair, judgement of major findings possible; 1=poor with definite diagnosis not possible. In the case of a discrepancy between reader 1 and reader 2 for the standard MRI a consensus decision was reached and this consensus decision in conjunction with the clinical assessment was used as the gold standard.

Statistics

Statistical analysis was carried out with SPSS version 20.0 (SPSS Inc., Chicago, IL, USA). Differences in image quality and diagnostic confidence between the standard MRI and Hr-TOF MRA were calculated by the Wilcoxon signed rank test. Differences in distribution regarding categorical variables, such as risk factor profiles, were analysed using Fisher's exact test. A standard 4×4 contingency table was used to calculate the sensitivity, specificity, positive predictive value, negative predictive value and the accuracy. Interobserver agreement and agreement between standard MRI and Hr-TOF MRA were tested using Cohen's

Table 2 MR parameters

	T1w	T1w	CE-MRA	CE-MRA	TOF
Field strength (Tesla)	1.5	3	1.5	3	3
Sequence	2D-TSE	2D-TSE	3D	3D	3DGRE
ECG gating	None	None	None	None	None
Fat suppression	Yes	Yes	None	None	Yes
TR (ms)	853	840	3.7	4.2	21
TE (ms)	16	8.4(cor)/10.9(ax)	1.5	1.5	3.96
PAT factor	–	–	–	2	2
ETL	1	5	1	1	NA
Flip angle (°)	90	90	25	20	25
Averages	1	1	1	1	1
FOV (mm^2)	320×160	320×320	320×160	300×300	160×120
Matrix	320×160	320×320	384×192	300×300	240×320
Number of slices	19	23	88	120	114
Slice thickness (mm)	3.5	3.0	0.8	1.2	1.0
Pixel size (mm^2)	1.0×1.0	1.0×1.0	0.84×0.84	1.0×1.0	0.5×0.5
Imaging time per slice (s)					
Coronal	12.0	10.4	NA	NA	
Axial	12.4	9.1			2.6
Imaging time per sequence (min)					
Coronal	3:49	4:00	0:30	0:36	
Axial	3:55	3:30			4:57
Flow suppression	No	No	No	No	Inflow suppression (veins)

CE contrast enhanced, *Hr-TOF* high-resolution time-of-flight, *TSE* turbo spin echo, *ECG* electrocardiogram, *TR* time to repetition, TE time to echo, *PAT* parallel acquisition technique, *ETL* echo train length, *FOV* field of view, *NA* not applicable

kappa test. The degree of stenosis determined by standard MRI and Hr-TOF MRA was correlated by using Spearman's correlation coefficient *R*. Results were considered to be statistically significant if the calculated *P* value was less than 0.05.

Results

Patients

Twenty consecutive patients with cDISS fulfilled the inclusion criteria. Table 1 gives an overview of the demographics, clinical presentation and cardiovascular risk factors. The mean age of all patients was 45.4 years, range 24–66 years. Dissections were found in 11 men and 9 women. The average age of the men was significantly higher than the mean age of the women (51.6±1 SD vs. 37.8±1 SD years; $P<0.001$). Women were significantly more likely to present with multiple dissections than men (6 women vs. 2 men; $P=0.037$). Of our 20 patients 12 suffered a stroke (5 men, 7 women), 1 patient had Horner syndrome and 7 patients had non-specific symptoms, such as headache or neck pain.

MR imaging

The mean time between the standard MRI and the Hr-TOF MRA was 4.5±2.7 days with a range of 0–8 days.

Image quality and diagnostic confidence

Image quality of standard MRI was rated slightly higher than the image quality of Hr-TOF MRA (3.2±0.50 vs. 2.9±0.62; $P=0.02$). Diagnostic confidence did not differ significantly and was 3.0±0.73 for Hr-TOF MRA and 3.2±0.76 for standard MRI; $P=0.27$.

Arterial dissections

On the basis of the consensus decision of the standard MRI, 30 dissected arteries were found: 13 patients had 1 dissection (11 in the internal carotid artery, 2 in the vertebral artery), 4 patients had 2 dissections (4 in the internal carotid artery, 4 in the vertebral artery), 3 patients had 3 dissections (3 in the internal carotid artery, 6 in the vertebral artery). Typical examples are depicted in Figs. 1, 2, 3 and 4.

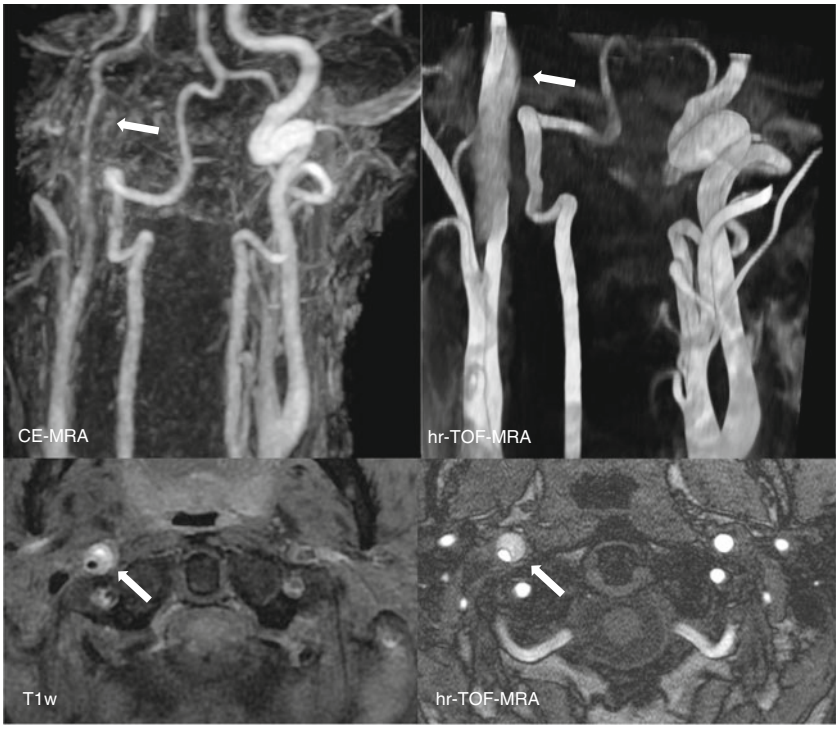

Fig. 1 Restricted lumen and wall haematoma (*arrow*) in an arterial dissection in the right common carotid artery, which is hyperintense on time-of-flight (TOF) and slightly hyperintense on T1w images. The intimal flap is clearly visible on axial TOF images. Maximum intensity projection (MIP) reconstruction of contrast-enhanced magnetic resonance angiography (CE-MRA) shows the stenosis in the area of the vessel wall haematoma. On MIP reconstruction of the Hr-TOF MRA the vessel diameter appears dilated which is due to the high signal intensity of the vessel wall haematoma

Reader 1 found 30 cDISS in the reading of the Hr-TOF MRA. He missed 1 cDISS in the vertebral artery and identified one "false-positive" cDISS on Hr-TOF images in the carotid artery that was missed on the standard MRI. Reader 2 found 30 cDISS. He missed 2 cDISS in the vertebral artery and identified 2 "false-positive" cDISS, 1 in the carotid artery and 1 in the vertebral artery on Hr-TOF images that was missed on the standard MRI (Table 3).

Compared with the standard MRI, this resulted in sensitivity, specificity, positive and negative predictive values and accuracy of reader 1 of 0.97, 0.98, 0.97, 0.98 and 0.97

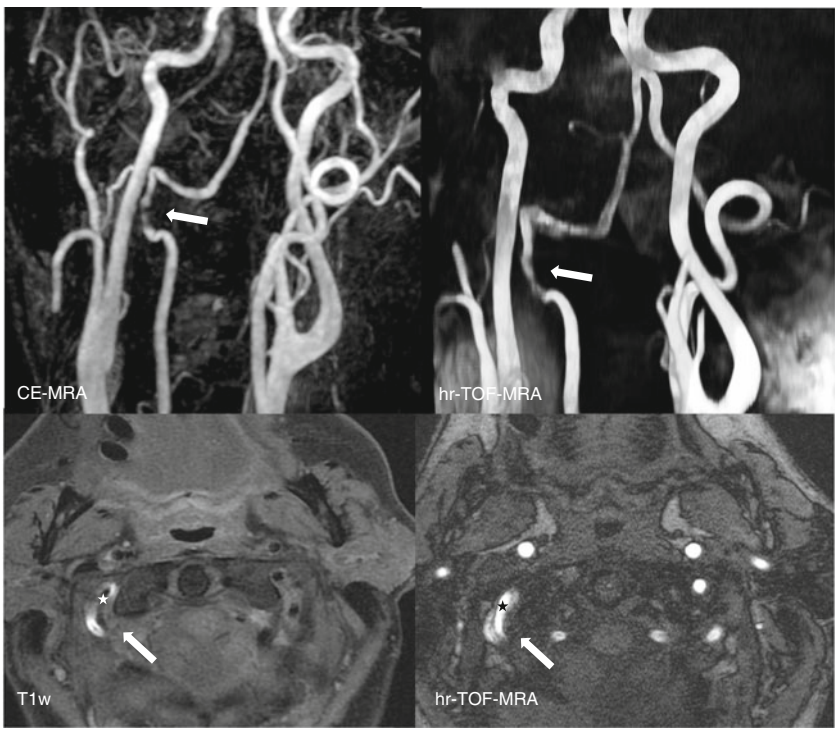

Fig. 2 Axial T1w images with fat suppression and axial TOF images. The *arrow* points to an arterial dissection in the V_3 segment of the right vertebral artery that is hyperintense on TOF and T1w images. The arterial lumen (*asterisk*) is hypointense on T1w and hyperintense on TOF images, which might make it easier to detect the dissection on T1w images. However, the intimal flap/dissected membrane is clearly identified on TOF images. Coronal images are MIP reconstructions

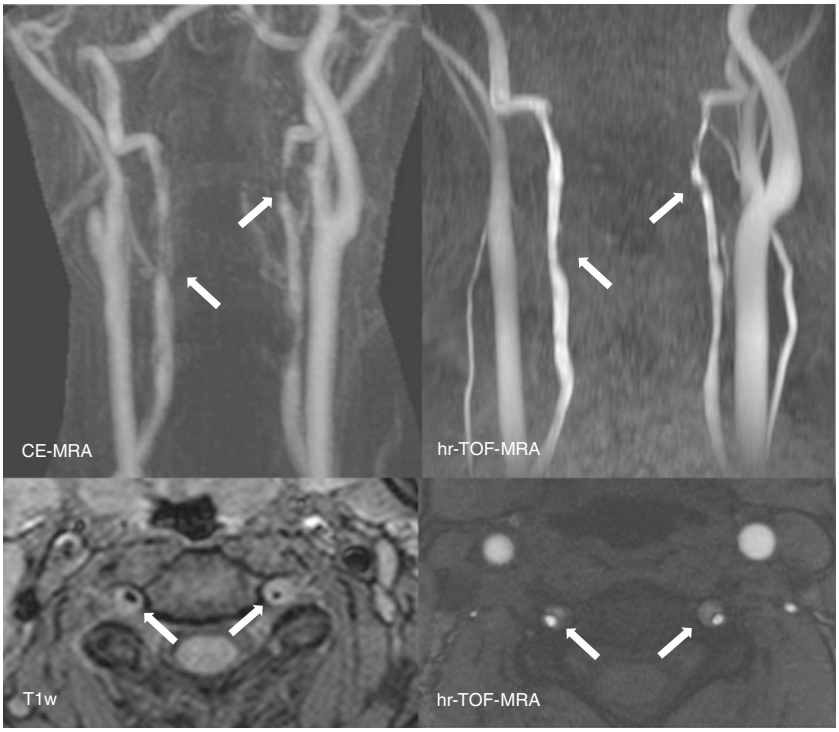

Fig. 3 MIP reconstructions of Hr-TOF MRA and contrast-enhanced MRA show wall irregularities in the vertebral arteries. The *arrows* point to hyperintense regions on fat-suppressed T1w and TOF images, consistent with arterial dissections in the V_2 segments of both vertebral arteries. TOF images also visualise the intimal flap/dissection membrane, which is hypointense compared with the lumen and the vessel wall haematoma

and a Cohen's kappa value of 0.95 ($P<0.001$). Calculated values for sensitivity, specificity, positive and negative predictive values and accuracy of reader 2 were 0.93, 0.96, 0.93, 0.96 and 0.95. This resulted in a Cohen's kappa value of 0.89 ($P<0.001$). Interobserver agreement of the readers was strong with a Cohen's kappa value of 0.89 for Hr-TOF ($P<0.0001$).

Stenosis assessment

On the basis of the consensus decision of the standard MRI, 10 out of 80 vessels (12.5 %) were occluded. On the basis of Hr-TOF MRA both reviewers correctly identified 9 out of 10 occluded vessels (Cohen's kappa compared with standard MRI=0.94, $P<0.001$). One occlusion of the carotid

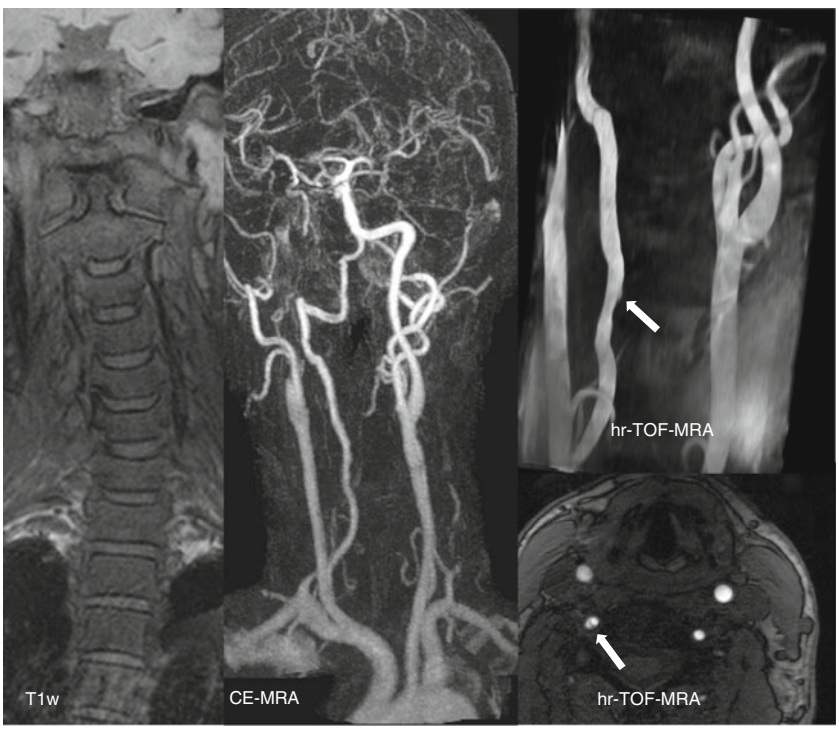

Fig. 4 A 44-year-old female patient with occlusion of the right carotid artery due to an arterial dissection (not shown). Another small dissection of the V_2 segment of the right vertebral artery was only visible on the axial Hr-TOF MRA but not on the coronal T1w images of this region (axial T1w images of this region were not acquired). Coronal images are MIP reconstructions

Table 3 Cross table: number of dissections

Reviewer 1/Reviewer 2		MRI standard	
		Dissection	No dissection
HR-TOF	Dissection	28/26	1/2
	No dissection	1/2	50/50

Hr-TOF high-resolution time-of-flight

artery was classified as a high-grade stenosis on Hr-TOF MRA by both reviewers. Interobserver agreement for assessment of occlusion by Hr-TOF MRA was perfect with a Cohen's kappa value of 1.00 ($P<0.001$). There was a strong correlation for quantitative stenosis estimates between Hr-TOF MRA and standard MRI with a correlation coefficient of 0.96 for reader 1 and 0.90 for reader 2. Furthermore, there was strong agreement between readers 1 and 2 when the degree of stenosis was assessed using the Hr-TOF MRA, with $R=0.91$ ($P<0.001$). The mean degree of stenosis of the dissected vessels was 66.9 % (±24.4) on Hr-TOF MRA and 63.5 % (±29.3) on standard MRI ($P=0.27$).

Discussion

Owing to their high diagnostic accuracy, non-invasive techniques have essentially replaced conventional diagnostic catheter angiography for imaging the arterial vasculature. Contrast-enhanced MRA in combination with fat-suppressed T1w images currently represents the preferred approach for the non-invasive imaging of arterial dissections [7, 15]. The association between gadolinium chelate administration in the renally impaired and NSF has raised increasing concerns about the safety of contrast-enhanced MR techniques [9]. CE-MRA for the evaluation of arterial dissections is particularly problematic given the high concurrent incidence of renal impairment. Thus, there has been an increased impetus to develop unenhanced MR techniques of comparable accuracy and efficiency to the standard contrast-enhanced MRI [16].

This study demonstrated that the use of unenhanced Hr-TOF MRA of the carotid and vertebral arteries is able to diagnose cDISS with good to excellent sensitivity and specificity compared with standard MRI consisting of a CE-MRA and fs T1w images in coronal and axial planes. In our opinion Hr-TOF MRA has two potential clinical applications:

1. Replacement of the standard protocol with contrast medium in patients with known or suspected kidney disease
2. An additional sequence in patients in whom the standard sequences fail to reach sufficient image quality for diagnostic purposes, e.g. suboptimal contrast bolus, or movement artefacts.

On the basis of our own experience [14], the combination of the head coil and the surface coil restricts motion substantially, thus providing sufficient image quality in most cases. Suboptimal bolus timing may also reduce CE-MRA image quality. Nevertheless overall image quality was still rated slightly higher on standard MRI compared with Hr-TOF MRA. However, there were no differences in the diagnostic confidence of the two imaging techniques. One advantage of Hr-TOF MRA is that this technique provides angiographic information and information on the vessel wall simultaneously. Hr-TOF MRA also provides T1 contrast and most of the vessel wall haematomas in our study were bright on T1 and Hr-TOF images, suggesting the presence of early or late subacute haematomas [17]. Interestingly, two dissections were detected on Hr-TOF images that were not seen with the standard protocol, suggesting that Hr-TOF images might be more sensitive than conventional sequences. However, Hr-TOF images were acquired with substantially higher resolution and had a smaller slice thickness than conventional T1w images, which may in part explain the higher number of arterial dissections detected on Hr-TOF images. Furthermore, the additionally detected cDISS on Hr-TOF images did not change the clinical regimen in these patients as all patients included in this study had at least one dissection and therapy does not differ between patients with one cDISS or those with more than one cDISS. However, it would be desirable to use Hr-TOF MRA in a prospective study in combination with a standard MRI in order to evaluate whether additional cDISS can be detected on Hr-TOF images in patients in whom standard MRI is negative.

Our study showed relatively strong agreement for the assessment of stenosis and vessel occlusion between Hr-TOF MRA and standard MRI. However, Hr-TOF MRA failed to identify one occluded vessel but did not tend to underestimate the degree of stenosis compared with the standard MRI. This is consistent with the literature [18], in which CE-MRA did not offer a significant advantage over TOF MRA in distinguishing surgically treatable internal carotid stenosis. On the other hand Kollias et al. found TOF MRA unsuccessful (owing to motion artefacts) compared with contrast-enhanced MR angiography [19]. Nevertheless, the grading of the degree of stenosis was not the main purpose of our study and there is an extensive body of literature that compares different MR methods for grading arterial stenosis [16, 20].

With regard to limitations, in our study the standard MRI in combination with the clinical examination was used to establish the gold standard for the diagnosis of cDISS. While this could potentially lead to the under- or over-

diagnosis of arterial dissections this approach is considered to be the clinical standard as histological data of arterial dissections is not available and MRI is better suited to detecting the vessel wall haematoma than other imaging techniques, such as CT angiography or conventional DSA.

Our imaging criteria for the diagnosis of cDISS in the standard protocol were hyperintense signal on fat-suppressed T1w sequences and stenosis or occlusion at contrast-enhanced MR angiography. Thus small dissections which did not cause any luminal narrowing might have been missed in the standard protocol. Furthermore, all of our patients had a cDISS and we did not include a true control group without cDISS in our study. For statistical comparison we used vessels without cDISS as controls. Furthermore, all values calculated for sensitivity, specificity, NPV and PPV refer to the comparison of two imaging methods and not to the clinical diagnosis of cDISS.

Hr-TOF images did not cover the proximal portion of the vertebral and common carotid arteries. Although primary arterial dissection rarely originates in this region, such lesions would have been missed on Hr-TOF images alone.

The Hr-TOF MRA and the standard MRI were not acquired on the same day; therefore changes in signal intensity due to decomposition of the vessel wall haematoma as described by Habs et al. [17] might have biased our results. The time between the standard MRI and the Hr-TOF MRI was 8 days and it is therefore possible that dissections occurred during this time period and we cannot know for certain whether Hr-TOF MRA would be equally useful as the standard protocol at the initial time of presentation. However, the best time at which to diagnose and detect cDISS on MRI is unclear although our own experience in imaging cDISS indicates that hyperacute and acute haematomas—which are iso- to hypointense on T1w images—are more difficult to detect than early or late subacute haematomas which are hyperintense on T1w images.

In conclusion, our results suggest that Hr-TOF MRA might be a viable alternative to contrast-enhanced MRA techniques in diagnosing arterial dissection, allowing an accurate MR-based assessment of the carotid and vertebral arteries without the need for administration of gadolinium-based contrast agents. This would be a major benefit especially in patients with impaired renal function and a potentially elevated risk of NSF development or in patients in which the standard MRI fails to achieve diagnostic image quality.

References

1. Baumgartner RW, Bogousslavsky J (2005) Clinical manifestations of carotid dissection. Front Neurol Neurosci 20:70–76
2. Rist PM, Diener HC, Kurth T, Schürks M (2011) Migraine, migraine aura, and cervical artery dissection: a systematic review and meta-analysis. Cephalalgia 31:886–896
3. Debette S, Markus HS (2009) The genetics of cervical artery dissection: a systematic review. Stroke 40:e459–e466
4. Rubinstein SM, Peerdeman SM, van Tulder MW, Riphagen I, Haldeman S (2005) A systematic review of the risk factors for cervical artery dissection. Stroke 36:1575–1580
5. Guillon B, Berhet K, Benslamia L, Bertrand M, Bousser MG, Tzourio C (2003) Infection and the risk of spontaneous cervical artery dissection: a case–control study. Stroke 34:e79–e81
6. Pfefferkorn T, Saam T, Rominger A, Habs M, Gerdes LA, Schmidt C, Cyran C, Straube A, Linn J, Nilolaou K, Bartenstein P, Reiser M, Hacker M, Dichgans M (2011) Vessel wall inflammation in spontaneous cervical artery dissection: a prospective, observational positron emission tomography, computed tomography, and magnetic resonance imaging study. Stroke 42:1563–1568
7. Bachmann R, Nassenstein I, Kooijman H, Dittrich R, Kugel H, Niederstadt T, Kuhlenbäumer G, Ringelstein EB, Krämer S, Heindel W (2006) Spontaneous acute dissection of the internal carotid artery: high resolution magnetic resonance imaging at 3.0 tesla with a dedicated surface coil. Invest Radiol 41:105–111
8. Oppenheim C, Naggara O, Touzé E, Lacour JC, Schmitt E, Bonneville F, Crozier S, Guégan-Massardier E, Gerardin E, Leclerc X, Neau JP, Sirol M, Toussaint JF, Mas JL, Méder JF (2009) High-resolution MR imaging of the cervical arterial wall: what the radiologist needs to know. Radiographics 29:1413–1431
9. Thomsen HS (2006) Nephrogenic systemic fibrosis: a serious late adverse reaction to gadodiamide. Eur Radiol 16:2619–2621
10. Naggara O, Soares F, Touze E, Roy D, Leclerc X, Pruvo JP, Mas JL, Meder JF, Oppenheim C (2011) Is it possible to recognize cervical artery dissection on stroke brain MR imaging? A matched case–control study. AJNR Am J Neurodadiol 32:869–873
11. Naggara O, Louillet F, Touzé E, Roy D, Leclerc X, Mas JL, Pruvo JP, Meder JF, Oppenheim C (2010) Added value of high-resolution MR imaging in the diagnosis of vertevral artery dissection. AJNR Am J Neuroradiol 31:1707–1712
12. Bouthillier A, van Loveren HR, Keller JT (1996) Segments of the internal carotid artery: a new classification. Neurosurgery 38:425–433
13. Hayes CE, Mathis CM, Yuan C (1996) Surface coil phased arrays for high-resolution imaging of the carotid arteries. J Magn Reson Imaging 6:109–112
14. Saam T, Raya JG, Cyran CC, Bochmann K, Meimarakis G, Dietrich O, Clevert DA, Frey U, Yuan C, Hatsukami TS, Reiser MF, Nikolaou K (2009) High resolution carotid black-blood 3T MR with parallel imaging and dedicated 4-channel surface coils. J Cardiovasc Magn Reson 11:41
15. Nassenstein I, Krämer SC, Niederstadt T, Stehling C, Dittrich R, Kuhlenbäumer G, Ringelstein EB, Heindel W, Bachmann R (2005) Incidence of cerebral ischemia in patients with suspected cervical artery dissection: first results of a prospective study. RoFo 177:1532–1539
16. Kramer H, Runge VM, Morelli JN, Williams KD, Naul LG, Nikolaou K, Reiser MF, Wintersperger BJ (2011) Magnetic resonance angiography of the carotid arteries: comparison of unenhanced and contrast enhanced techniques. Eur Radiol 21:1667–1676
17. Habs M, Pfefferkorn T, Cyran CC, Grimm J, Rominger A, Hacker M, Opherk C, Reiser MF, Nikolaou K, Saam T (2011) Age determination of vessel wall hematoma in spontaneous cervical artery dissection: a multi-sequence 3T cardiovascular magnetic resonance study. J Cardiovasc Magn Reson 13:76
18. Babiarz LS, Romero JM, Murphy EK, Brobeck B, Schaefer PW, Gonzalez RG, Lev MH (2009) Contrast-enhanced MR

angiography is not more accurate than unenhanced 2D time-of-flight MR angiography for determining>or=70% internal carotid artery stenosis. AJNR Am J Neuroradiol 30:761–768

19. Kollias SS, Binkert CA, Ruesch S, Valavanis A (1999) Contrast-enhanced MR angiography of the supra-aortic vessels in 24 seconds: a feasibility study. Neuroradiology 41:391–400
20. Hirookas R, Ogasawara K, Inoue T, Fujiwara S, Sasaki M, Chida K, Ishigaki D, Kobayashi M, Nishimoto H, Otawara Y, Tsushima E, Ogawa A (2011) Simple assessment of cerebral hemodynamics using single-slab 3D time-of-flight MR angiography in patients with cervical internal carotid artery steno-occlusive diseases: comparison with quantitative perfusion single-photon emission CT. AJNR Am J Neuroradiol 30:559–563